CHAPTER 1

Elementary Reactions: Rate Constants and their Temperature-Dependence

IAN W. M. SMITH

University Chemical Laboratories, UK, Lensfield Road, Cambridge CB2 1EW, UK
Email: iwms2@cam.ac.uk

1.1 Introduction

This chapter considers the kinetics of elementary reactions. Unlike complex reactions, elementary reactions cannot be subdivided into processes of lesser molecular complexity, whereas complex reactions proceed through a network of elementary reactions. Elementary reactions necessarily involve the participation of a small integral number of atoms and/or molecules, and one can further define them by saying that the chemical change involves molecular processes which mimic the chemical equation that is used to represent the reaction. Thus, the reaction

$$F + H_2 \rightarrow HF + H \qquad (R1)$$

occurs in binary collisions—though not all binary collisions—between fluorine atoms and molecules of di-hydrogen.

Elementary chemical reactions can be classified as collisional or decay processes. The former, of which reaction (R1) is an example, are generally referred to as bimolecular; two species (*e.g.* F and H_2) collide in each microscopic event

RSC Theoretical and Computational Chemistry Series No. 6
Reaction Rate Constant Computations: Theories and Applications
Edited by Keli Han and Tianshu Chu

Published by the Royal Society of Chemistry, www.rsc.org

that leads to reaction and the formation of products (*e.g.* HF and H). Decay processes are unimolecular: chemical change occurs in processes where single molecules either dissociate to two new chemical species or isomerise, that is, change to a different form with the same chemical formula.

However, it is necessary to insert a cautionary note in the description of unimolecular processes as elementary since this designation disguises the fact that, although the elementary processes in which chemical change occurs are indeed unimolecular, they involve molecules of reactants that contain high internal energy compared with the great majority. Consequently, collisions in which energy is transferred but no chemical change occurs also play a vital role in the kinetics of these reactions. Finally, I note that association reactions are the reverse of dissociation reactions. They involve two reactant species, frequently two free radicals, coming together to form a collision complex, which is subsequently stabilised against re-dissociation—usually by collision with a third species which removes energy from the energised complex. In the limit of the reactants being atoms, for example, pairs of oxygen atoms, the lifetime of the diatomic complex is very short and the stabilising collision is essentially simultaneous with the radical–radical collision. In this case, the reaction can be considered as termolecular.

Reactions occurring in solution are inevitably affected to a greater or lesser degree by the close proximity of solvent molecules to the reactants. Consequently, one can argue that, by definition, elementary reactions only take place in the gas phase. Certainly, such reactions are simpler to treat theoretically. In this chapter, I shall consider only gas-phase reactions. For such reactions, a continuing synergy between experiment and theory has brought forth a remarkable improvement in our understanding, especially of the factors that influence the magnitude of rate constants and their dependence on temperature, and also of the dynamics of such reactions, that is, what factors control the motions of the atoms as chemical bonds rearrange and reactants are converted to products.

The improvement in our knowledge and understanding of elementary chemical reactions has been stimulated by two principal drivers. The first is the developments in experimental techniques and the ability to apply them over an ever-widening range of temperatures, coupled to a massive increase in computing power which has, *inter alia*, allowed potential energy surfaces to be calculated accurately for elementary reactions of increasing complexity (see section 1.3). The second driver has been the wish to model complex chemical environments: (a) in planetary atmospheres, especially that of Earth; (b) at high temperatures in pyrolytic and combustion systems; and (c) in interstellar and circumstellar media. The computer models contain a large number of ordinary differential equations in each of which the change with time of a particular chemical species (X) is represented as the difference in the sum of the rates of the elementary reactions in which X is formed and the sum of the rates of the elementary reactions in which X is consumed, that is:

$$\frac{dX}{dt} = \sum rates\ of\ formation\ processes - \sum rates\ of\ removal\ processes \quad (1.1)$$

The temperatures in the three types of system, (a), (b) and (c), vary widely, from up to several thousand K in (a) to as low as 10 K in (c), emphasising the need either for measurements over a correspondingly wide range of temperatures, or for theoretical methods capable either of calculating the rate constants over similar ranges of temperature or, at least, of extrapolating the values of the experimental rate constants that may have been determined over a limited range of temperatures—or even a single temperature—to the temperatures appropriate to the models of a particular environment.

1.2 A Little History

The systematic study of chemical kinetics, that is, of the rates of chemical reactions and their dependence on temperature, dates back to the middle of the 19th century. During the next 60 years, a number of expressions were proposed to express the temperature-dependence of the rate constant, $k(T)$. These efforts have been reviewed by Laidler,[1] who pointed out the difficulty of distinguishing between the various proposals of how $k(T)$ varies with temperature when the available values of $k(T)$ cover only a small temperature range. After the early years of the 20th century, attention focused on what is generally referred to as the Arrhenius equation:

$$k(T) = A \exp(-E_{act}/RT) \tag{1.2}$$

where A is best referred to as the pre-exponential factor and E_{act} is the activation energy, and a modified form of this equation in which additional temperature-dependence is allowed for in the pre-exponential term:

$$k(T) = A' T^m \exp(-E'_{act}/RT) \tag{1.3}$$

These equations came to be favoured over other temperature-dependent expressions for the rate constant largely because, in Laidler's words, the other expressions were 'theoretically sterile', whereas eqn (1.2) could be rationalised on the basis of the reactants requiring some minimum amount of energy to undergo reaction.

Although the title of eqn (1.2) honours Arrhenius, its origin was in the work of van't Hoff,[2] who generously acknowledged still earlier work by Pfaundler.[3] Van't Hoff appreciated that, at equilibrium, the rate of forward and reverse reactions become equal so that the ratio of the rate constants, $k_f(T)$ and $k_r(T)$, for these reactions is equal to the equilibrium constant; *i.e.*

$$k_f(T)/k_r(T) = K_c(T)^{\dagger} \tag{1.4}$$

[†]The subscript $_c$ to K_c and ΔU_c° indicates that the standard states for these quantities are unit concentration and not the thermodynamic standard pressure of 1 bar.

Combining this equation with that from chemical thermodynamics which bears van't Hoff's name:

$$d\ln K_c(T)/dT = \Delta U_c^{o}/RT^2 \tag{1.5}$$

yields

$$d\ln k_f(T)/dT - d\ln k_r(T)/dT = \Delta U_c^{o}/RT^2 \tag{1.6}$$

Van't Hoff then argued that the temperature-dependence of the rate constants $k_f(T)$ and $k_r(T)$ is influenced by two different energies, E_f and E_r, whose difference corresponds to ΔU_c^{o}, so that:

$$d\ln k_f(T)/dT = E_f/RT^2 \tag{1.7a}$$

and

$$d\ln k_r(T)/dT = E_r/RT^2 \tag{1.7b}$$

Van't Hoff recognised that ΔU_c^{o} is generally *not* independent of temperature. Of course, if it is, integrating either eqn (1.7.a) or (1.7b) recovers the Arrhenius equation (eqn (1.2)). Arrhenius's contribution[4] to this debate was to note that the effect of temperature on chemical reaction rates was much too large to be the result of changes in the translational energies of the reactants and, in a postulate reminiscent of transition state theory (see below), he suggested that an equilibrium is established between reactant molecules and 'active' ones that could react without further input of energy. If this equilibrium mirrors that for chemical equilibrium, and hence obeys an equation like eqn (1.5), then one obtains eqn (1.2).

More generally, it can be seen that eqn (1.6) can be used to obtain an expression for a temperature-dependent activation energy (and imply a temperature-dependent pre-exponential factor), usually written as:

$$E_{act}(T) = -\,d\ln k(T)/d(1/RT) \tag{1.8}$$

The modified form of the Arrhenius equation given in eqn (1.3) was apparently first suggested by Kooij,[5] a student of van't Hoff's. If that equation is operated on according to eqn (1.8), one obtains the following expression for the activation energy:

$$E_{act}(T) = E_{act}^{'} + mRT \text{ and } A = A'(Te)^m \tag{1.9}$$

In tables of rate constants, compiled for the purposes of combustion, atmospheric and astrochemical modelling, the recommended rate constants are often expressed using the following form of the Kooij equation:

$$k(T) = \alpha(T/T^{o})^{\beta}\exp(-\gamma/T) \tag{1.10}$$

where it is sensible to view α, β and γ simply as parameters that define the temperature-dependence of a particular rate constant. Moreover, it should be noted that, because of correlations between these parameters, they are only accurately determined when $k(T)$ has been measured (or calculated) accurately over a wide range of temperature.

Finally in this section, I refer to the insight into the activation energy provided by Tolman.[6a,b] This depends on the notion that for collisions between reactants at a specific relative velocity, u, one can define a rate coefficient as the product of u and the reaction cross-section, $\sigma(u)$, with the result that the thermal rate constant, $k(T)$, can (in principle) be found by first multiplying $u\sigma(u)$, by a normalised function, $f(u; T)$, describing the distribution of relative velocities at temperature T, and then integrating the resulting expression over u:[7]

$$k(T) = \int u\sigma(u) f(u\,; T) du \tag{1.11}$$

This equation can be rewritten in terms of relative translational energies, $E_{trans} = \frac{1}{2}\mu u^2$ where μ is the collisional reduced mass, yielding:

$$k(T) = (1/\pi\mu)^{1/2}(2/k_{\mathrm{B}}T)^{3/2} \int_{E^{o}_{trans}}^{\infty} \sigma(E_{trans}) E_{trans} \exp(-E_{trans}/RT) dE_{trans} \tag{1.12}$$

where the lower limit of integration, $E^{o}_{trans,}$ is the threshold energy.

Tolman's contribution was to realise that, if eqn (1.12) is substituted into the right-hand side of eqn (1.8), one finds that:

$$E_{act} = \langle E_{trans,reac} \rangle - \langle E_{trans} \rangle \tag{1.13}$$

That is the activation energy is the difference between the average translational energy in the collisions that lead to reaction and the average translational energy in all collisions. Although this treatment neglects any dependence of the reactivity on the internal states of the reactants, it demonstrates the important result that rate constants can *decrease* with temperature if the average collisional energy in reactive collisions is less than that in all collisions. This provides a rationale for the observation of negative activation energies for some reactions.

1.3 Potential Energy Surfaces and Transition State Theory

Within the Born–Oppenheimer approximation, the results of molecular collisions depend on the motion of the nuclear particles (atoms) on the potential energy (hyper) surface (PES) that describes how the electronic energy of the

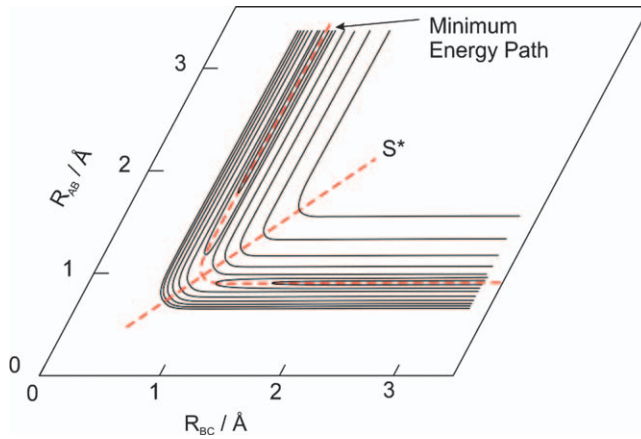

Figure 1.1 Contour line plot of a potential energy surface (PES) for reaction between three identical atoms (A, B, C) based on that for the $H + H_2$. The diagram also shows the minimum energy path (MEP) and the 'critical dividing line' (S*). The axes are 'skewed' so that a trajectory can be visualised as the motion of a single mass point across this PES.

system depends on the relative position of the nuclei.[‡] (Remember that the derivatives of the PES with respect to the nuclear co-ordinates describe the forces acting on the atoms at any position on the PES.) In addition, dynamic and kinematic factors will determine the result (or, quantum mechanically, the probability of a given result) for any particular collision.

The calculation of a PES from first principles quantum mechanics is a formidable task, not least because it requires many individual calculations for different geometries if the PES is to be fully mapped. Even the simplest reactive system of interest involves three atoms, which I shall refer to as $\boldsymbol{A}$, $\boldsymbol{B}$ and $\boldsymbol{C}$, and requires three spatial co-ordinates, say $\boldsymbol{r_{AB}}$, $\boldsymbol{r_{BC}}$, and $\boldsymbol{r_{CA}}$, to define its instantaneous geometry. The potential energy can then be written as $\boldsymbol{V}(\boldsymbol{r_{AB}}, \boldsymbol{r_{BC}}, \boldsymbol{r_{CA}})$ and the difficulty or 'expense' of the quantum chemical calculation of $\boldsymbol{V}$ at any single geometry depends strongly on the number of electrons in the system. From this point of view, a system of three H atoms is the simplest involving neutral atoms. A surface representing $\boldsymbol{V}(\boldsymbol{r_{AB}}, \boldsymbol{r_{BC}}, \boldsymbol{r_{CA}})$ for three collinear atoms can be represented by the kind of contour plot shown in Figure 1.1. Imposing linearity means that $\boldsymbol{V}$ depends on only two independent co-ordinates so that $\boldsymbol{V}$ can be represented by a surface. Lifting this restriction so that $\boldsymbol{V}$ depends on three independent spatial co-ordinates means that a hypersurface is required.

A full characterisation of $\boldsymbol{V}(\boldsymbol{r_{AB}}, \boldsymbol{r_{BC}}, \boldsymbol{r_{CA}})$ may be required for full scattering calculations, for example, for quasi-classical trajectory calculations.[8] What might be termed traditional scattering calculations proceed through three stages. First,

[‡]This description refers to reactions occurring adiabatically on the ground state PES. Photochemical reactions frequently involve motion on more than one PES and consideration must be given to 'surface-hopping'.

the energies at points on the PES are calculated by full quantum chemical methods, at a level of theory that is appropriate, or which can be afforded. Then these energies are fitted to a function that describes how V depends on the position co-ordinates of the system, and finally one calculates, by classical or quantum methods, the dynamics of collisions on the fitted PES. Monte Carlo methods can be used to select the initial parameters (position and momentum co-ordinates) for each collision in order to yield statistically meaningful results in a reasonably small sample of trajectories. Such calculations yield quantities such as scattering angles, product state distributions, *etc.,* that is, the quantities that are measured to characterise the reaction dynamics of the reaction under examination.

To examine the collisional dynamics, an alternative method to that just described can be implemented. In this method, V and the corresponding forces acting on the atoms are calculated at each point along a trajectory as it evolves.[9] This method, known as direct dynamics, has the advantage that no time is wasted calculating V at geometries distant from those through which reactive trajectories proceed, that is, distant from the minimum energy path (MEP) for the reaction. However, electronic structure calculations are expensive in computer time and such calculations must be performed many times for each trajectory. Furthermore, they have to be carried out for a sample of trajectories that is sufficiently large to yield results that are statistically meaningful. Consequently, it is not possible to use electronic structure calculations of the highest accuracy (and cost) in direct dynamics calculations.

Fortunately, if one's objective is to determine 'only' rate constants, one can employ transition state theory (TST), which has been comprehensively reviewed by Fernandez-Ramos *et al.*[10] In TST, attention is focused on the flux of trajectories through a critical dividing surface (or strictly, critical dividing hypersurface), S^*, which divides the phase space associated with reactants from that associated with products. In most cases, the location of S^* can be defined by just the positional co-ordinates of the system; that is, in our example involving just three atoms $S^*(r_{AB}, r_{BC}, r_{CA})$. For reactions involving N atoms and with a well-defined maximum on the MEP, a normal mode analysis at this potential energy barrier will generally yield $(3N - 6)$ force constants (or $(3N - 5)$ if the atoms are collinear), one of which will be negative. The direction of motion associated with this negative force constant (that is, for which the curvature is negative) defines the reaction co-ordinate and $S^*(r_{AB}, r_{BC}, r_{CA})$ is orthogonal to this direction. If TST is to be applied to a particular reaction, electronic structure calculations can first be used to define the MEP, and then higher level calculations performed close to any barrier that is found along the MEP in order to define accurately the energies and structures at these barriers.

TST rests on a number of assumptions. Three of these would apply if the motions of the nuclear particles could be described by classical dynamics. They are:

- The Born–Oppenheimer approximation is valid.
- The reactant molecules are distributed amongst their states according to the Maxwell–Boltzmann laws.

- The transition state serves as a dynamical bottleneck such that once trajectories reach this bottleneck they pass through it to products without any turning back so that there is no re-crossing of the critical dividing surface.

Tests[11] comparing the results of classical trajectories with those of classical TST demonstrate that the third of these conditions is satisfied at collision energies close to the threshold energy, so that TST estimates of the rate constant are exact. At higher energies, the effects of re-crossing lower the reactive flux through $\boldsymbol{S}^*$ below the total flux and TST provides an upper bound to the true rate constant.

Of course, a great strength of TST is that quantum effects can be incorporated into the estimates of $k(T)$. Then there are two more implicit assumptions in conventional (and canonical) TST:

- Quantum effects associated with motions orthogonal to the reaction co-ordinate can be included by replacing classical partition functions in the expression for $k(T)$ by quantum mechanical partition functions (see below), and quantum effects associated with motion along the reaction co-ordinate can be included by estimating a factor, $\kappa(T)$, to allow for quantum mechanical tunnelling through the barrier.
- The dynamical bottleneck can be identified (as introduced above) by a surface $\boldsymbol{S}^*$ in co-ordinate space which is orthogonal to the reaction co-ordinate.

With these assumptions, the expression for the rate constant for a bimolecular reaction between reactants $\boldsymbol{R_1}$ and $\boldsymbol{R_2}$ can be written:

$$k(T) = \sigma\kappa(T)\left(\frac{k_B T}{h}\right)\left(\frac{(q/V)_{R_1R_2^{\neq}}}{(q/V)_{R_1}(q/V)_{R_2}}\right)\exp\left(-\Delta E_0^{\neq}/k_B T\right) \qquad (1.14)$$

In this equation, σ allows for the number of equivalent reaction paths, for example, $\sigma = 4$ for $H + CH_4$, $(q/V)_i$ is the 'per volume' partition function for the specified species (i), $^{\neq}$ denotes the transition state species, and $\Delta E_0^{\neq}$ is the difference in energy between the zeroth levels in the transition state and in the reactants, sometimes referred to as the vibrationally adiabatic barrier.[§] It should be noted[7] that, because of zero-point effects, the energy of the classical barrier, $\boldsymbol{V}^*$, is related to but not the same as $\Delta E_0^{\neq}$ and that, because the pre-exponential term on the right-hand-side of eqn (1.14) depends on temperature, $\Delta E_0^{\neq}$ is also not identical with E_{act} as defined in eqn (1.8).

Eqn (1.14) can be rearranged by factoring out the translational partition functions, leaving a 'per unit volume' partition function associated with the

[§]In this formulation of the TST expression for $k(T)$, the vibrational partition functions are referred to the appropriate zero-point levels, so that, within the harmonic approximation, $q_{vib} = \prod_s (1 - \exp(-h\omega_s/k_B T))^{-1}$, the product is over the s vibrations of the species.

relative translational motion of $\boldsymbol{R_1}$ and $\boldsymbol{R_2}$ in terms of the collisional reduced mass, $\mu = m_{\boldsymbol{R_1}} m_{\boldsymbol{R_2}}/(m_{\boldsymbol{R_1}} + m_{\boldsymbol{R_2}})$:

$$k(T) = \sigma\kappa(T)\left(\frac{k_B T}{h}\right)\left(\frac{h^2}{2\pi\mu k_B T}\right)^{3/2}\left(\frac{(q_{int})_{R_1R_2^{\neq}}}{(q_{int})_{R_1}(q_{int})_{R_2}}\right)\exp\left(-\Delta E_0^{\neq}/k_B T\right) \tag{1.15}$$

In this equation, $(q_{int})_i$ is the partition function associated with the internal degrees of freedom (rotations and vibrations) of species i. In addition, the $(q_{int})_i$ can be written as products of vibrational $(q_{vib})_i$ and rotational $(q_{rot})_i$ partition functions. It is also instructive to write $(q_{vib})_{\boldsymbol{R_1R_2}^{\neq}}$ as the product of terms associated with the 'conserved' modes, which correlate with vibrational modes in the reactants, and the 'transitional' modes, which correlate with relative translational and rotational motions in the reactants. Then:

$$\left(\frac{(q_{int})_{R_1R_2^{\neq}}}{(q_{int})_{R_1}(q_{int})_{R_2}}\right) = \left(\frac{(q_{rot})_{R_1R_2^{\neq}}}{(q_{rot})_{R_1}(q_{rot})_{R_2}}\right)\left(\frac{(q_{cons\ vib})_{R_1R_2^{\neq}}\ (q_{trans\ vib})_{R_1R_2^{\neq}}}{(q_{vib})_{R_1}(q_{vib})_{R_2}}\right) \tag{1.16}$$

For reactions where $\boldsymbol{R_1}$ and $\boldsymbol{R_2}$ are both diatomic and the reaction proceeds through a linear transition state, there will be six vibrations in the transition state of which two will be 'conserved' and are likely to have high frequencies, close to those for the vibrations in $\boldsymbol{R_1}$ and $\boldsymbol{R_2}$, whereas the other four vibrations are 'transitional' and will be low frequency 'bending' modes. The partition functions $(q_{cons\ vib})_{\boldsymbol{R_1R_2}^{\neq}}$, $(q_{vib})_{\boldsymbol{R_1}}$ and $(q_{vib})_{\boldsymbol{R_2}}$ will all have values close to unity, so the second term on the right-hand side of eqn (1.16) reduces, to a good degree of approximation, to $(q_{trans\ vib})_{\boldsymbol{R1R2}^{\neq}}$. The vibrations contributing to this partition function in the case specified will be two pairs of degenerate bending modes with low frequencies. To evaluate these partition functions, it is often necessary to take account of the anharmonicities associated with these motions.

The evaluation of the tunnelling factor, $\kappa(T)$, has been a subject of much debate in the literature and is related to the separability of the motion along the reaction co-ordinate from the motions orthogonal to the reaction co-ordinate.[10] Inclusion of a tunnelling factor is especially important in those bimolecular reactions where an H-atom is transferred, *e.g.* $OH + CH_4 \rightarrow H_2O + CH_3$. Reactions of this type are important in the Earth's atmosphere[¶] and in combustion systems. The first stage in estimating values of $\kappa(T)$ is to find the MEP in properly scaled and skewed co-ordinates.[12] These co-ordinates are used in the plot of the PES for three collinear atoms shown in Figure 1.1. They make appropriate allowance for the masses of the atoms, so that a trajectory can be visualised as the motion of a particle of unit mass (or mass μ) over the PES. The next stage is to calculate the zero-point energies associated with the motions orthogonal to this MEP, not just at the barrier but also along the MEP. This

[¶]The oxidation of alkanes in the Earth's atmosphere is initiated by reactions of this type with hydroxyl radicals.

operation yields a vibrationally adiabatic potential on which the barrier may be significantly different from that on the classical MEP. Finally, allowance needs to be made for the fact that, because of inertial effects and the motions in the vibrations orthogonal to the MEP, trajectories do not actually follow the MEP. In particular, tunnelling trajectories may 'cut the corner' on the PES, burrowing through the 'shoulder' of the critical dividing surface, rather than passing over, or through, the minimum barrier, $\boldsymbol{V}^*$.[10]

Once a vibrationally adiabatic potential has been calculated, it becomes possible to examine whether the transition state is truly located at the potential energy barrier $\boldsymbol{V}^*$. To do this one needs to calculate the frequencies and zero-point energies associated with modes orthogonal to the reaction path ($\boldsymbol{s}$). One can then use eqn (1.15) to estimate the TST rate constant for each of these generalised transition states along $\boldsymbol{s}$. This procedure is employed in variational transition state theory (VTST).[10] Remembering that the properly selected transition state should be the 'bottleneck' on the PES (that is, the location which minimises the reactive flux), the proper choice of the transition state should be that which leads to the minimum estimate of the rate constant. In general, for a reaction with a well-defined barrier, the variational transition state for a reaction of reactants in their vibrational ground state is not likely to differ much from that obtained by choosing the dividing surface to be orthogonal to the reaction co-ordinate at the maximum on the classical MEP. This situation can, however, change if one uses VTST to estimate rate constants for reactions of vibrationally excited reactants—especially if the vibrational excitation is in the bond that is broken in the reaction.[13a,b] To calculate the thermal rate constant, $k(T)$, strictly rate constants should be calculated for each combination of reactant vibrational states and the thermally weighted values of these rate constants should be summed to find $k(T)$. In practice, except at high temperatures, the contribution of reaction from vibrationally excited reactant states will be very small.

Up to this point I have described the development of TST for a canonical assembly of molecules, that is, to the situation where the distribution of reactant molecules among states is defined by the Boltzmann laws and a single temperature. It has been implicitly assumed that the location of the transition state (or critical dividing surface) is independent of the energy of the reactants. However, the microcanonical version of TST, referred to as μTST can provide estimates of the rate coefficients, $k(E)$, for reactants of defined energy, and by integrating these values of $k(E)$ over the thermal distribution of energies, provide an improved estimate of $k(T)$.

Microcanonical TST has found wide application in the case of unimolecular reactions at the limit of high pressure (see below). In this situation, the translational partition functions for the reactants and transition state species are identical, so that eqn (1.14) for the canonical rate constant simplifies to:

$$k(T) = \sigma\kappa(T)\left(\frac{k_B T}{h}\right)\left(\frac{(q_{int})_{R_3^{\neq}}}{(q_{int})_{R_3}}\right)\exp\left(-\Delta E_0^{\neq}/k_B T\right) \qquad (1.17)$$

where $\boldsymbol{R}_3$ is the reactant undergoing reaction through a transition state denoted by $\boldsymbol{R}_3^{\neq}$.

The microcanonical rate constant is given by:

$$k(E) = \sigma\,\kappa(E)\;\frac{N^*(E-V)}{h\,\rho(E)} \tag{1.18}$$

In this equation, $N^*(E - V)$ is the number of internal states in the transition state with energies between the internal energy E and the potential energy V on the MEP and $\rho(E)$ is the density of internal energy states in the reactant at energy E. Microcanonical TST can be applied in a variational form (μVTST) by evaluating eqn (1.18) at various points along the MEP and taking the lowest value of $k(E)$ as the best estimate of the rate coefficient.

For bimolecular reactions, it is necessary to include the density of reactant states (*i.e.* the number per unit volume per energy interval) associated with the relative translational motion:

$$\rho(E_{trans}) = \frac{\mu\,(\mu E_{trans})^{1/2}}{2^{1/2}\,\hbar^3\,\pi^2} \tag{1.19}$$

where μ is the collisional reduced mass and E_{trans} is the energy associated with relative translational motion. The total density of states is obtained by multiplying $\rho(E_{trans})$ by the number of internal states in the same energy interval.

TST, as described so far, is applicable when there is a significant energy barrier along the MEP. However, it has been increasingly recognised that many bimolecular reactions occur over PESs where there is no such barrier. One important class comprises those between ions and neutral molecules, which are important in the chemistry of low-temperature environments, as found in the cold cores of dense interstellar clouds.[14] The long-range electrostatic attractive forces are relatively strong and, if the neutral species is non-polar, they depend only on the distance (R) separating the two species and arise between the charge (e) on the ion and the dipole induced in the molecule. An effective potential can be defined by adding to the intermolecular electrostatic potential the (conserved) energy associated with the orbital angular momentum, $(J(J+1))^{\frac{1}{2}}\hbar$, yielding (in c.g.s. units):

$$V_{eff}(\boldsymbol{R}) = [J(J+1)\hbar^2/\mu R^2] - \alpha e^2/2R^4 \tag{1.20}$$

where α is the polarisability of the molecule and μ is the collisional reduced mass. The rate of reaction is often determined by the ability of these forces to bring the reactants into close contact, a process frequently referred to as 'capture'. One can obtain an expression for the cross-section for close collisions by: (i) finding the value of R (R_{max}) at which $V_{eff}(R)$ has its maximum value (by differentiating the right-hand-side of eqn (1.20) and setting the result equal to zero); (ii) finding the corresponding value of $V_{eff}(R)$, that is, $V_{eff}(R_{,max})$; and (iii) using these results to find the maximum value of J (or equivalently the

maximum impact parameter) for which collisions with relative energy E_{trans} can 'surmount' the centrifugal barrier, $V_{eff}(R_{max})$. Finally, one can obtain a rate constant for close collisions by multiplying the expression for the cross-section by the Maxwell–Boltzmann expression for the distribution of relative velocities and integrating the result.[12]

The procedure outlined in the previous paragraph yields a very simple, and temperature-independent, expression for the rate constant:

$$k(T) = 2\pi e\ (\alpha/\mu)^{1/2} \tag{1.21}$$

When the molecule is polar, so that there are ion–dipole as well as ion-induced dipole forces between the reactants, expressions have been recommended that 'correct' eqn (1.21).[14] The estimated rate constants are increased, especially at low temperatures, so that $k(T)$ exhibits a negative temperature-dependence.[15]

Georgievskii and Klippenstein proposed a 'long-range transition state theory', which can estimate the rate constant for mutual capture of two neutral species.[16] For a number of reasons, the situation is generally more complicated than in the case of ion-neutral systems; the intermolecular forces are weaker and act over a shorter range, and directional forces, for example, derived from dipole–dipole forces, dipole–quadrupole forces, *etc*. are often pre-dominant. The theory is variational and is implemented both at an energy and angular momentum resolved level, and is given the acronym μJ-VTST. For each combination of E and J, it is necessary to calculate an average rate coefficient for different reactant orientations, which can be done using Monte Carlo methods. As Georgievskii and Klippenstein point out, this long-range TST is likely to work best at very low temperatures. At higher temperatures, the transition state moves to shorter reactant separations and effects such as chemical bonding and steric repulsion should be considered (see below for further discussion).

Finally in this section, I emphasise that one result of the increasing sophistication and accuracy of *ab initio* quantum chemical calculations is that they show that the PESs and MEPs for many bimolecular reactions exhibit several turning points (maxima and minima). A classic case of this is the reaction between NH_2 and NO. Experiments have shown that this reaction is rapid, $k(298\ \mathrm{K}) = 1.7\times10^{-11}\ \mathrm{cm^3\ molecule^{-1}\ s^{-1}}$, and that its principal products at low temperatures are $N_2 + H_2O$.[17] This result is remarkable given the number of bonds that must break and form for this transformation. Nor is this result of simply academic interest, since the reaction is the key process in the Thermal De-NO_x process in which NH_3 is added to the exhaust gases from an internal combustion engine to remove NO_x (NO and NO_2). Figure 1.2 shows the reaction paths for this reaction,[18] which shows that there are only 'submerged barriers'[‖] along the paths leading from $NH_2 + NO$ to $N_2 + H_2O$. In addition, a number of cases have been treated—and some are considered later in this

[‖]By the term 'submerged barrier', sometimes referred to as a 'reef', I mean an energy maximum along the MEP, but one whose energy is below that of the separated reactants.

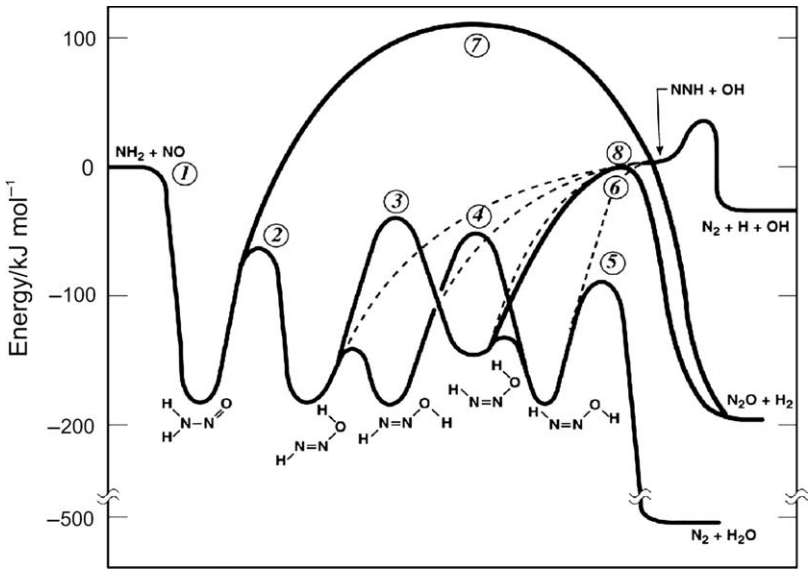

Figure 1.2 Profile of the potential energy along the minimum energy path for the reaction between NH_2 and NO, showing the maxima and minima along the path leading to the major products, $N_2 + H_2O$.
(Reproduced, with permission, from ref. 18.)

chapter—by TST calculations that consider the controlling effects of 'outer' and 'inner' transition states, passage through the outer one being treated by long-range TST and passage through the inner one by more conventional TST.

1.4 Comparisons between Experimental and Theoretical Results for Selected Reactions

In this section, for a number of selected reactions, I compare the results of kinetic experiments with those of theoretical calculations, especially those using transition state methods. A disproportionately large fraction of the reactions selected are those that my colleagues and I have worked on in the past. The other criteria for inclusion have been to select reactions for which rate constants have been measured over a wide range of temperature, and which exhibit non-Arrhenius behaviour. Although in the previous section I have emphasised bimolecular reactions, I choose to start this comparison of experimental and theoretical data by considering unimolecular reactions.

1.4.1 Dissociation and Association Reactions

Dissociation reactions occur by a unimolecular mechanism, that is, the crucial stage in which a reactant is transformed into (usually two) products involves single molecules breaking or re-arranging their bonds. Most dissociation

reactions fall into one of two categories, depending on whether the products are molecules or free radicals. Well-studied examples of each category include:

$$C_2H_5Cl \rightarrow C_2H_4 + HCl \qquad (R2)$$

$$HONO_2 \rightarrow OH + NO_2 \qquad (R3)$$

Isomerisation reactions such as:

$$CH_3NC \rightarrow CH_3CN \qquad (R4)$$

also occur by a unimolecular mechanism.

The fundamental mechanism for unimolecular reactions was proposed 90 years ago by Lindemann. Besides the unimolecular reactive step involving reactants with internal energy (E_{int}) sufficient to bring about the chemical change, he proposed that collisions with any species (***M***) present could convert reactant molecules (***A***) into critically energised reactant molecules (***A****) (that is, molecules with E_{int} greater than the minimum internal energy for reaction) and remove internal energy from ***A**** thereby converting them to molecules with insufficient internal energy to react:

$$\boldsymbol{A} + \boldsymbol{M} \rightarrow \boldsymbol{A}^* + \boldsymbol{M} \qquad (1.22)$$

$$\boldsymbol{A}^* + \boldsymbol{M} \rightarrow \boldsymbol{A} + \boldsymbol{M} \qquad (1.-22)$$

$$\boldsymbol{A}^* + \boldsymbol{M} \rightarrow \boldsymbol{products} \qquad (1.23)$$

To find the rate of formation of the products from ***A**** molecules with specified internal energy E_{int}, one equates the rate of production of such molecules by process (1.22) to their rate of removal by (1.–22) and (1.23), and then writes the rate of reaction as the product of the rate coefficient for reaction of ***A**** molecules with internal energy E_{int} and the steady-state concentration of these critically energised molecules. This procedure yields the following expression for the rate of reaction:

$$\frac{d[products]}{dt} = \frac{k_{reac}(E_{\text{int}})\,\{k_a(E_{\text{int}})/k_{-a}(E_{\text{int}})\}}{1 + \{k_{reac}(E_{\text{int}})/k_{-a}(E_{\text{int}})[M]\}}\,[A] \qquad (1.24)$$

where $k_a(E_{int})$, $k_{-a}(E_{int})$ and $k(E_{reac})$ are the rate coefficients for (1.22), (1.–22) and (1.23). This equation is the microscopic equivalent of the Lindemann–Hinshelwood equation. It defines a phenomenological first-order rate coefficient:

$$k(E_{\text{int}}) = \frac{k_{reac}(E_{\text{int}})\,\{k_a(E_{\text{int}})/k_{-a}(E_{\text{int}})\}}{1 + \{k_{reac}(E_{\text{int}})/k_{-a}(E_{\text{int}})[M]\}} \qquad (1.25)$$

To derive a thermal rate constant, one must solve the equation:

$$k(T) = \int_{E^{o}_{\mathrm{int}}}^{\infty} k(E_{\mathrm{int}})\, dE_{\mathrm{int}} \tag{1.26}$$

In the limit $[M] \rightarrow \infty$, often referred to as the 'high pressure limit', a combination of Eqs. (1.25) and (1.26) simplifies to:

$$k^{\infty}(T) = \int_{E^{o}_{\mathrm{int}}}^{\infty} k_{reac}(E_{\mathrm{int}})\, \{k_a(E_{\mathrm{int}})/k_{-a}(E_{\mathrm{int}})\}\, dE_{\mathrm{int}} \tag{1.27}$$

Physically, collisions of ***A*** and ***A**** with ***M*** are frequent and the distribution of reactant molecules over internal energy states is not disturbed by the occurrence of reaction. Consequently, TST can be applied. The TST expression for the rate constant is given earlier in eqn (1.17).

Dissociation reactions to molecular products, such as reaction (R2), and isomerisation reactions, such as reaction (R4), are characterised by high energy, well-defined,[††] barriers and therefore high activation energies. Because the rate constants vary strongly with temperature, it is difficult to study these reactions over a wide range of temperature. For example, the classic experiments of Schneider and Rabinovitch[19] on the isomerisation CH_3NC to CH_3CN were carried out at three temperatures, 472.5 K, 503.5 K and 532.9 K, but over several orders of magnitude in total pressure, that is, $[M]$. In these types of reaction, the temperature dependence of the rate constants is dominated by the exponential term in eqn (1.17); any effect of a variation in the pre-exponential factor with temperature is relatively too small to observe. In the limit of high pressure, the activation energy was measured[19] to be 160.1 kJ mol^{-1}. The decomposition of C_2H_5Cl to $C_2H_4 + HCl$, reaction (R2), has been studied several times. Robinson and Holbrook[20] list the pre-exponential factors (A^{∞}) and activation energies ($E^{\infty}{}_{act}$) that have been measured in the limit of high pressure: the values of $E^{\infty}{}_{act}$ range from 236 to 254 kJ mol^{-1}, compared with the change in internal energy for the reaction of ΔU^{o}(298 K) of + 69.7 kJ mol^{-1}.

Further information about the nature of these reactions can be obtained by considering the magnitude of the pre-exponential factors, A^{∞}. For reaction (R4), $A^{\infty} = 4 \times 10^{13}\,\mathrm{s}^{-1}$ and for reaction (R2), $A^{\infty} = 4 \times 10^{12}\,\mathrm{s}^{-1}$. These values, especially the one for the isomerisation of CH_3NC, are close to those for $(k_B T/h)$ for the temperatures used in the experiments. According to eqn (1.17), this means that the partition functions associated with the internal motions in the reactant and in the transition state are similar, demonstrating that the transition state is 'tight', in contrast (see below) to those for most dissociation reactions that lead to radical products, like reaction (R3). In terms of the

[††]By 'well-defined' I mean that there is a maximum along the reaction path at a significantly higher energy than those of both the reactant and product species.

thermodynamic formulation of TST,[12] the entropies of activation for reactions (R2) and (R4) are small.

In contrast to the reactions considered so far, for reactions in which a single bond is broken to create two radicals, such as reaction (R3), there is usually no 'well-defined' maximum on the MEP leading from reactant to products, though on occasions there is a submerged barrier between the main minimum on the PES and a shallow minimum associated with the operation of long-range forces. In these cases, the transition states can be classified as 'loose'; their location will depend on E_{int} and J, the orbital angular momentum, and a microcanonical form of TST should be employed to estimate the rate constants. A second way in which such reactions differ from those with well-defined barriers is that rate constants can be measured, or derived, over a wide temperature range. This can be done by studying the kinetics of dissociation at high temperatures and those for association at low temperatures, eqn (1.4) connecting the rate constants for the forward and reverse reactions can then be used, together with thermodynamic data, to find the rate constants for both reactions over the full range of temperature.

Before discussing the kinetics of association reactions in more detail, it is necessary to point out that their mechanism, like that for dissociation reactions, involves three steps. Thus, for the association of two radicals $\boldsymbol{Rad}_1$ and $\boldsymbol{Rad}_2$, there are steps involving the formation and re-dissociation of an energised complex, $(\boldsymbol{Rad}_1\boldsymbol{Rad}_2)^{*\ddagger\ddagger}$, and a step in which energy is removed from $(\boldsymbol{Rad}_1\boldsymbol{Rad}_2)^*$ in collisions with the bath gas $\boldsymbol{M}$, creating the stable product $\boldsymbol{Rad}_1\boldsymbol{Rad}_2$:

$$\boldsymbol{Rad}_1 + \boldsymbol{Rad}_2 \rightarrow (\boldsymbol{Rad}_1\boldsymbol{Rad}_2)^* \tag{1.28}$$

$$(\boldsymbol{Rad}_1\boldsymbol{Rad}_2)^* \rightarrow \boldsymbol{Rad}_1 + \boldsymbol{Rad}_2 \tag{1.-28}$$

$$(\boldsymbol{Rad}_1\boldsymbol{Rad}_2)^* + \boldsymbol{M} \rightarrow \boldsymbol{Rad}_1\boldsymbol{Rad}_2 \tag{1.29}$$

If we again apply the steady-state approximation to find the concentration of $(\boldsymbol{Rad}_1\boldsymbol{Rad}_2)^*$, we obtain an equation for the rate of formation of stabilised products, $\boldsymbol{Rad}_1\boldsymbol{Rad}_2$:

$$\frac{d[Rad_1Rad_2]}{dt} = \frac{k_{ass}(E_{\text{int}})}{1 + \{k_{diss}(E_{\text{int}})/k_M[M]\}}\,[Rad_1][Rad_2] \tag{1.30}$$

where $k_{ass}(E_{int})$, $k_{diss}(E_{int})$ and k_M are the rate coefficients for processes (1.28), (1.–28) and (1.29).[§§] This equation is equivalent to eqn (1.24) derived for dissociation and it defines a phenomenological second-order rate coefficient:

$$k(E_{\text{int}}) = \frac{k_{ass}(E_{\text{int}})}{1 + \{k_{diss}(E_{\text{int}})/k_M[M]\}} \tag{1.31}$$

[‡‡]This complex contains, as internal energy, energy that is released as the $\boldsymbol{Rad}_1$–$\boldsymbol{Rad}_2$ bond forms.
[§§]Here k_M is assumed to be independent of the internal energy of $(\boldsymbol{Rad}_1\boldsymbol{Rad}_2)^*$; this is often referred to as 'the strong collision assumption'.

As before, the thermal rate constant can be obtained by integration of the energy-dependent rate coefficient over the appropriate thermal distribution Here, I focus on the behaviour in the high pressure ($[M]\rightarrow\infty$), and low pressure ($[M]\rightarrow 0$) limits. In the limits of high and low pressure, eqn (1.31) reduces to:

$$k^{\infty}(E_{int}) = k_{ass}(E_{int}) \text{ and } k^{0}(E_{int}) = \{k_{ass}(E_{int})/k_{diss}(E_{int})\}k_{M}\{M\} \qquad (1.32a, 1.32b)$$

In the limit of high pressure, collisions maintain the thermal distribution of reactant molecules over their internal energy states and consequently TST can be used to determine the thermal rate constants for dissociation and association. However, in the case where there is no maximum in the reaction path leading from reactants to products, it is necessary to take account of angular momentum (J) constraints as well as internal energy. The transition state is not found at a single separation but rather it depends on E_{int} and J. Then, in the language of the statistical adiabatic channel model (SACM),[21] the partition function for the transition state can be expressed as:[22]

$$(q_{\text{int}})_{R_3^{\#}} = \sum_{J=0}^{\infty}(2J+1)\int_{0}^{\infty} N^{*}(E,J)\,\exp\left(-\frac{(E-E_0)}{k_BT}\right)\frac{dE}{k_BT} \qquad (1.33)$$

$N^*(E,J)$ is the number of 'open channel states', that is, states with total angular momentum J and with energy less than E_0, which is the threshold energy of individual reactive channels. As Troe comments,[22] the central problem in applying this theory is 'the determination of the energy pattern of the channel threshold energies'. In principle, the calculation of the channel energies would be carried out *ab initio*, that is, using quantum mechanical methods. In practice, Troe has given semi-empirical formulae for the variation in energy of the channel potentials. In practice, the values of $k^{\infty}(T)$ for association reactions of two radicals are frequently found to be close to the value that might be estimated from a simple capture theory with due allowance for the fact that the radical reactants may correlate with more than PES. Furthermore, in keeping with what might be expected from a simple capture approach, the values of $k^{\infty}(T)$ show, at most, a mild dependence on temperature.

In the low pressure limit, $k^0(T)$, the rate constant for dissociation is given by eqn (1.27) and that for association by taking the thermal average of the expression on the right-hand side of eqn (1.32b). In the latter case, the values of $k^0(E_{int})$—and $k^0(T)$—depend chiefly on the internal energy or, in canonical systems, the temperature and the number of atoms in $\boldsymbol{Rad_1Rad_2}$. The greater the number of atoms, the smaller the magnitude of $k_{diss}(E_{int})$ or $k_{diss}(T)$, because there are more vibrations over which the internal energy that is released as $\boldsymbol{Rad_1}$ and $\boldsymbol{Rad_2}$ combine can be distributed. In addition, the higher E_{int} (or T), the sooner sufficient energy will relocate in the $\boldsymbol{Rad_1}$–$\boldsymbol{Rad_2}$ bond and break it.

To estimate the rate constant for association in the limit of low pressure, one can use the canonical form of eqn (1.32b). Incorporating the strong collision assumption, one can write:

$$k^0_{ass}(T) = k_M\{M\}\left\{q_{(\boldsymbol{Rad}_1\boldsymbol{Rad}_2)^*}/q_{\boldsymbol{Rad}_1}q_{\boldsymbol{Rad}_2}\right\} \quad (1.34)$$

Here, it is important to note that $q_{(\boldsymbol{Rad}_1\boldsymbol{Rad}_2)^*}$ is the partition function per unit volume for the energised complexes formed by the recombination of the radicals $\boldsymbol{Rad}_1$ and $\boldsymbol{Rad}_2$. The corresponding equation for the rate constant for dissociation in the limit of low pressure is:

$$k^0_{diss}(T) = k_M\{M\}\left\{q_{(\boldsymbol{R}_1\boldsymbol{R}_2)^*}/q_{\boldsymbol{R}_1\boldsymbol{R}_2}\right\}\exp(-\Delta E_0/k_{\mathrm{B}}T) \quad (1.35)$$

Troe[23] has described how one can estimate the value of the partition function $q_{(\boldsymbol{R1R2})^*}$. One begins with a basic expression for the density of internal states at the dissociation limit, which treats the vibrations in $(\boldsymbol{Rad}_1\boldsymbol{Rad}_2)^*$ as harmonic. Multiplicative factors are then estimated to allow, in turn for: (i) the anharmonicity of the vibrations; (ii) the energy dependence of the density of vibrational states; (iii) an overall rotation factor, which allows for the existence of centrifugal barriers; and (iv) an internal rotation factor allowing for the barriers associated with internal rotors.

This method of Troe appears capable of reproducing experimentally determined rate constants to within a factor of about 2 or 3. Table 1.1 lists a few of the values of $k^0_{ass}(T)$ from ref. 23. These data demonstrate that the rate constants increase markedly with the size (number of atoms) of the system and they show a marked negative dependence on the temperature, which is steeper the larger the system.

Reaction (R3), the dissociation of nitric acid, has been studied in shock tube experiments[24a,b,c] at temperatures between 800 and 1400 K and at pressures between 0.6 and 30 bar. The reverse association of OH and NO_2 at lower temperatures has been studied experimentally many times, not least because of its importance in atmospheric chemistry.[25] The kinetics have been measured over a wide range of conditions: temperatures up to 600 K, pressures from 1 mbar to 1 kbar,[26a,b] and a variety of 'bath gases', $\boldsymbol{M}$, including air.[25] The conditions in most of these studies are in the 'fall-off regime' (that is,

Table 1.1 Third-order rate constants, $k^0_{ass}(T)/[\mathrm{Ar}]$, for selected association reactions assuming 'strong collisions', as estimated by Troe.[23]

Reaction	T/*K*	$\{k^0_{ass}(T)/[\mathrm{Ar}]\}/cm^6\ molecule^{-2}\ s^{-1}$
$CH_3 + CH_3 \rightarrow C_2H_6$	300	4.4×10^{-25}
	1500	1.1×10^{-28}
$HO + NO_2 \rightarrow HONO_2$	300	9.4×10^{-30}
	1200	9.7×10^{-32}
$O + NO \rightarrow NO_2$	300	1.0×10^{-31}
	1000	3.0×10^{-32}

intermediate between the limiting high and low pressure limits) and the procedures for fitting the 'fall-off curves' to extract values of the rate constants in the low and high pressure limits have been discussed several times in the literature, most recently by Troe.[27a,b] The interpretation of the results is also complicated by the association of OH and NO_2 to form peroxynitrous acid, HOONO.[25,26b] References to all of this work can be found in the evaluation by the IUPAC Subcommittee for Gas Kinetic Data Evaluation (www.iupac-kinetic.ch.cam.ac.uk). This panel recommends for the limited temperature range of 200–300 K:

$$k^0_{ass}(T) = 3.3 \times 10^{-30}(T/300)^{-3.0}[N_2]\,\mathrm{cm^3\ molecule^{-1}s^{-1}} \qquad (1.36)$$

Studies by Troe, Hippler and their co-workers[26ab] at temperatures between 250 and 400 K have been performed at very high pressures, so that only a short extrapolation is required to derive the high pressure rate constants. Based largely on these measurements, for temperatures between 200 and 400 K, the IUPAC panel recommend a temperature-independent value of:

$$k^\infty_{ass}(T) = 6 \times 10^{-11}\,\mathrm{cm^3\ molecule^{-1}\ s^{-1}} \qquad (1.37)$$

This value of $k^\infty_{ass}(T)$ can be combined with thermodynamic data for OH, NO_2 and HNO_3[28] to derive an Arrhenius expression for the thermal dissociation of HNO_3:

$$k^\infty_{diss}(T) = 8.5 \times 10^{16}\exp(-24430/T)\mathrm{s^{-1}} \qquad (1.38)$$

The high value of the pre-exponential factor, A^∞, compared with the values given earlier for the decomposition of C_2H_5Cl and the isomerisation of CH_3NC, reflects the 'loose' nature of the transition state in this reaction in which a single bond is broken and two radicals are formed.

The high pressure rate constants for a large number of radical–radical association reactions have been studied theoretically by Klippenstein, Harding, Miller and co-workers.[29–32] They have focused especially, but not exclusively, on the recombination of alkyl radicals, such as $CH_3 + CH_3$,[29] of resonance-stabilised radicals such as $C_3H_3 + C_3H_3$,[30] and of the association of H atoms with alkyl and aryl radicals such as $CH_3 + H$[31] and $C_6H_5 + H$.[31] These reactions are particularly important in high temperature systems and experimental information about their rate constants is limited, generally to room temperature and above.

Klippenstein and colleagues calculated rate constants for these barrierless reactions employing a method they termed 'variational reaction co-ordinate transition state theory' (VRC-TST). In this version of TST, 'variational' does not only refer to the procedure for finding the location of the transition state along the reaction co-ordinate, for each combination of energy (E) and total angular momentum (J), but also to a search for the optimum definition of the

reaction co-ordinate.[32] For example, the results from calculations using as the reaction co-ordinate (a) the length of the bond that is being formed and (b) the separation of the centres-of-mass of the two radicals have been compared. High quality quantum chemical methods were used to determine the values of the electronic potential energy at various positions along the reaction co-ordinate and to evaluate the number of accessible states $N(E,J)$ at different locations, so that the minimum in $N(E,J)$ is used to define the transition state.

The results of a variety of standard electronic structure methods have been compared.[33] The authors emphasise the importance of using a method that correctly reproduces the long-term potential and from the methods that they studied, they concluded that CASPT2 (complete active space second-order perturbation theory) is the preferred approach, not only for the calculation of electronic energies but also for obtaining the geometries along the reaction co-ordinate. Direct counting methods are employed to calculate the energy levels associated with the 'conserved' modes and phase space integrals are used to find the contributions of the internal rotations and low frequency transitional modes that correlate with translational and rotational motions in the separated reactants.

In general, the rate constants from VRC-TST calculations are in good agreement with the limited experimental data that are available, though allowance (which may introduce some uncertainty) often has to be made for the fact that the calculations yield the limiting high pressure rate constant, whereas the experiments, especially those at high temperature, do not reach this limiting value. For the recombination of CH_3 radicals,[29] calculations were carried out at separations from 5.5 Å to 1.9 Å for two definitions of the reaction co-ordinate. The results near room temperature were in good agreement with experiment and predicted a decrease of a factor of 1.7 in $k^{\infty}(T)$ as the temperature rises from 300 to 1700 K. This decrease was accompanied by a shortening in the radical separation in the transition state from about 4.0 Å at 300 K to about 3.0 Å at 1500 K. Georgievskii *et al.*[30] have calculated rate constants for the recombination of propargyl (C_3H_3) and allyl (C_3H_5) radicals, and for the cross reaction between C_3H_3 and C_3H_5. Again they found a negative temperature-dependence for the overall values of $k^{\infty}(T)$, but a stronger dependence for $C_3H_5 + C_3H_5$ than for $C_3H_3 + C_3H_3$.

Harding *et al.*[31] have used the VRC-TST treatment to examine the kinetics of the association of H atoms with several alkyl and aryl radicals. For these reactions, the calculated values of $k^{\infty}(T)$ are multiplied by 0.9 to allow for 're-crossing', that is, the immediate re-dissociation of the initially formed complexes. Results using two *ab initio* evaluations of the interaction energies are in good agreement. The rate constants are in good agreement with the limited experimental data. They decrease by a factor of 10 with increase in the size of the alkyl radical from CH_3 to $C(CH_3)_3$, reflecting the increase in steric hindrance. For all the reactions studied, $k^{\infty}(T)$ showed a mild increase with temperature, being represented by the form $k^{\infty}(T) = C\,T^n$, with n taking values between 0.13 and 0.32.

The reactions that have been discussed so far in this section occur adiabatically on their ground state PES. However, there are thermal reactions which are electronically nonadiabatic; the total electron spin changes going from reactants to products. The thermal dissociation of N_2O—and of the electronically similar molecules CO_2, OCS and CS_2—have been much studied. The ground states of these molecules are singlets (*i.e.* the total spin quantum number $S = 0$), but the lowest energy products are a singlet diatomic molecule and an atom in a triplet state ($S = 1$), for example:

$$N_2O(^1\Sigma) \rightarrow N_2(^1\Sigma_g^+) + O(^3P_J) \qquad \text{(R5)}$$

The products of these reactions correlate with three triplet PESs, $2^3A' + {}^3A'$, which are not bound and apparently cross the ground state PES some way above the energy of $N_2(^1\Sigma_g{}^+) + O(^3P)$. This can be inferred from kinetic data on this dissociation obtained in shock tube experiments between 1000 and 3000 K.[17] The activation energy derived from shock tube experiments at high pressure is $E_{act}{}^{\infty} = 242\ \text{kJ mol}^{-1}$, appreciably higher than the endothermicity of the reaction, $\Delta_r H^{\circ}{}_{298} = 167.1\ \text{kJ mol}^{-1}$. To decompose, N_2O molecules do not only have to acquire sufficient internal energy to cross from the singlet PES to a triplet PES, they also have to undergo an electronically nonadiabatic transition. This is reflected in a low pre-exponential factor for the reaction of $A^{\infty} = 9.9 \times 10^{12}\ \text{s}^{-1}$. The high barrier for the reverse reaction of reaction (R5) has a profound effect in atmospheric chemistry, since it ensures that oxygen atoms formed in the atmosphere combine with O_2 to form O_3, not with N_2 to generate N_2O.

1.4.2 Bimolecular Reactions

As with association and dissociation reactions, it is useful to consider the kinetics of bimolecular reactions in the context of how the potential energy varies along the MEP from reactants to products. Broadly speaking, the form of the MEP depends on the nature of the reactants: are one or both electrically charged or neutral, are one or both saturated or unsaturated 'molecules', are one or both free radicals? Reactions between molecules are characterised by high barriers; for example, the activation energy for the reverse of reaction (R2) is between 166 and 184 kJ mol^{-1}, calculated from the values of $\Delta U^{\circ}(298\ \text{K})$ (+ 69.7 kJ mol^{-1}) for the forward dissociation reaction and its activation energy (236 to 254 kJ mol^{-1}).

1.4.2.1 Reactions between Radicals and Saturated Molecules

Reactions between simple free radicals, atomic or molecular, and molecules, both saturated and unsaturated, play an important role in atmospheric and combustion chemistry, and have been widely studied both experimentally and theoretically. In the case of saturated molecules, the rate constants are generally (but not always, see below) characterised by small positive activation energies,

usually less than *ca.* 50 kJ mol^{-1}. Two good examples of this behaviour are the reactions of the radicals CN and C_2H with H_2:

$$CN + H_2 \rightarrow HCN + H \quad (R6)$$

$$C_2H + H_2 \rightarrow HCCH + H \quad (R7)$$

The extensive kinetic measurements on these reactions, from 300 to 3500 K in the case of (R6) and from 180 to 3000 K in the case of (R7), have been evaluated by Baulch *et al.*[17] They expressed their recommendations for the rate constants in terms of eqn (1.10) with $T^o = 300$ K, and found $\alpha = 5.0\times10^{-13}$ cm^3 molecule^{-1} s^{-1}, $\beta = 2.60$ and $\gamma = 960$ K for (R6), and $\alpha = 1.95\times10^{-12}$ cm^3 molecule^{-1} s^{-1}, $\beta = 2.32$ and $\gamma = 444$ K for (R7). Curves representing these functions are displayed in Figure 1.3.

Ju and colleagues have examined the kinetics of both these reactions using canonical VTST with small curvature tunnelling corrections. For CN + H_2,[34] they made use of a global many-body expansion PES calculated by ter Horst *et al.*[35] with a barrier of $V^* = 13.35$ kJ mol^{-1} which, with zero-point effects included, yields a value of $\Delta E_0^{\neq} = 14.6$ kJ mol^{-1}. Ju *et al.*[34] calculated rate constants in moderately good agreement with the experimental values, and found that tunnelling is only significant below *ca.* 200 K. For C_2H + H_2, Ju *et al.*[36] used two PESs, one modified from that calculated by Wang and Bowman,[37]and the other from their own *ab initio* calculations at the QCISD (T, full)/aug-cc-pVTZ//QCISD(full)/cc-pVTZ level of theory. For this reaction, they found a barrier height $V^* = 5.8$ kJ mol^{-1} and 'an effective barrier height', that is, $\Delta E_o^{\neq}$, of 9.6 kJ mol^{-1}. Curves representing the rate constants calculated using TST are compared in Figure 1.3 with curves representing the experimental results.

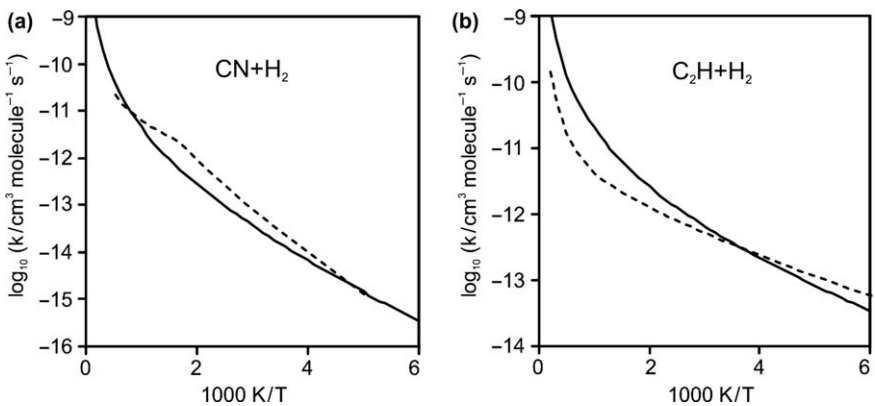

Figure 1.3 Comparison, for the reactions of CN (a) and C_2H (b) radicals with H_2, between the solid curves representing the fit to the experimentally determined rate constants,[17] and the dashed curves representing the results of transition state theory calculations.[34,36]

For both these exothermic reactions, the potential barriers are 'early', that is, 'reactant-like', in accordance with Polanyi's 'rules'.[38] One consequence is that the transitional modes in the transition states have low frequencies and the partition function for the internal modes in the transition state (see earlier, eqn (1.16)) will be strongly temperature-dependent, providing at least a partial reason for the positive temperature-dependence of the pre-exponential factor in the expressions for the rate constants.

Reactions (R6) and (R7) are examples of reactions which proceed along a MEP with a single maximum. (There will also be shallow minima associated with the van der Waals forces between the reactants and between the products.) There are, however, reactions between radicals and saturated molecules where the variation of energy along the MEP is more complex, and others where the van der Waals forces between the reactants play a role in determining the kinetic behaviour. An example of the second kind is the reaction between CN radicals and C_2H_6:

$$CN + C_2H_6 \rightarrow HCN + C_2H_5 \qquad (R8)$$

Rate constants have been measured at temperatures between 25 K[39] and 1500 K;[40] these results and others are shown in Figure 1.4. It can be seen that the rate constants pass through a minimum at *ca*. 200 K. This 'strange' behaviour has been explained by Georgievskii and Klippenstein[41] in terms of a 'two transition state model'. The outer transition state (or strictly transition states, as the location depends on E and J) are at separations where the interaction between the reactants is dominated by the long-range van der Waals forces; the inner transition state is at a separation smaller than that at the van der Waals minimum, where chemical forces start to act and a submerged barrier is created on the MEP. At low temperatures, passage through the outer transition state largely determines the rate constant and this can be treated by long-range TST; at higher temperatures, where the inner transition state starts to play a role, Georgievskii and Klippenstein[41] adopted a variational approach and corrected for anharmonic effects in the transitional modes. Their results are plotted in Figure 1.4; they obtained excellent agreement with the experimental results.

With my colleagues,[42a,b,43] I have used the two transition state model to examine the temperature-dependence of the rate constants for the reactions of CN[42ab] and CH[43] with NH_3. The work, both experimental and theoretical, has also enabled us to identify the major products of these reactions, which can therefore be written as:

$$CN + NH_3 \rightarrow HCN + NH_2 \qquad (R9)$$

$$CH + NH_3 \rightarrow H_2CNH + H \qquad (R10)$$

Both reactions proceed over rather complex MEPs which are shown in Figure 1.5, along with the experimental results at and below 300 K. The excellent agreement between the experimental values of $k(T)$ and the theoretical estimates of $k(T)$ for reaction (R9), and the moderately good agreement for reaction (R10) demonstrates the value of the two transition state approach

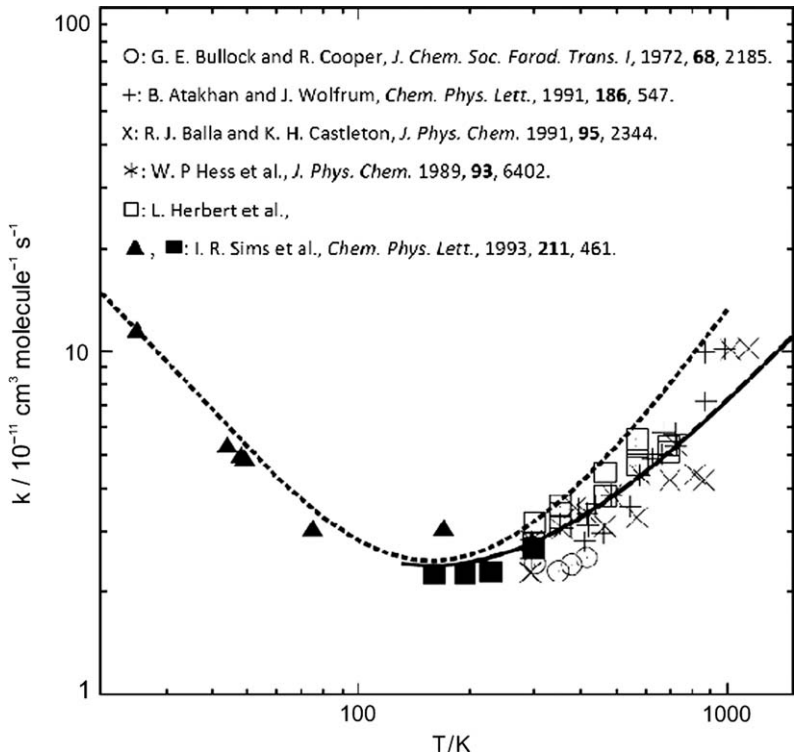

Figure 1.4 Comparison between the experimentally determined rate constants for the reaction between CN radicals and C_2H_6, and the results of two sets of transition state theory calculations. The dashed curve displays the results of TST calculation using the two transition state method, and the solid curve shows the results of VRC-TST calculations. Both these methods are described in the text.
(Adapted from Figure 9 in L. Herbert, I. W. M. Smith and R. D. Spencer-Smith, *Int. J. Chem. Kinet.*, 1992, **24**, 791.

when there is a submerged barrier on the MEP which is not too much lower than the reactant asymptote.

1.4.2.2 Reactions between Pairs of Free Radicals

Next I consider reactions where there is a single deep minimum along the MEP. Such an energy profile can be expected when two free radicals react. In the case of OH + NO_2, which was considered earlier, the potential energy on the ground state PES falls monotonically as the reactants approach, but there is no exit from the potential energy minimum at an energy lower than that leading back to reactants: radical association is the only mechanism for reaction. The reaction between $CN + O_2$ provides an example of another type of radical–radical reaction, which occurs when there is an exothermic route to two product species *via* a deep potential energy minimum. In such reactions, as in radical

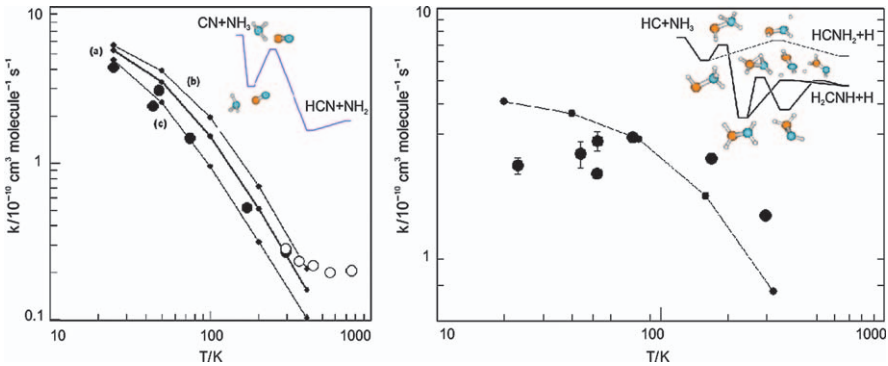

Figure 1.5 Comparisons between experimental results (●) and theoretical results (–•–) obtained using the two transition state approach (a) for $CN + NH_3$[42a] and (b) for $CH + NH_3$.[43] The calculations make use of the results of *ab initio* calculations of the MEP. For $CN + NH_3$, the fainter lines show the results of changing the energy of the inner transition state by $\pm 300\,cm^{-1}$ The inserts show the maxima and minima along the MEPs and the structures at these points on the PESs.

association reactions, the overall rate constant will be controlled by the transition states at long- or medium-range separation of the reactants. Upper limits to the rate constants can be estimated *via* the long-range TST approach of Georgievskii and Klippenstein,[16] with due allowance being made for the correlations of the reactants with more than one PES, not all of which will lead to reaction. In general, however, long-range TST and other approaches that only consider capture by the long-range van der Waals forces will overestimate the rate constant at anything but very low temperatures. In general, as the reactants approach and chemical forces start to act, the energy levels associated with the transitional modes become more widely spaced and, despite the decrease in the potential energy, the number of accessible energy levels (see eqn (1.18)) will decrease and lower the rate constant.

To illustrate this behaviour further, I consider the $CN + O_2$ reaction. The principal products of this reaction are $NCO + O$, though there is also a minor channel to $CO + NO$.

$$CN + O_2 \rightarrow NCO + O \qquad \text{(R11a)}$$

$$CN + O_2 \rightarrow CO + NO \qquad \text{(R11b)}$$

Measurements by Feng and Hershberger[44] show that the reaction yield of $CO + NO$ is 20%, and that of $NCO + O$ is 80%. Very probably both sets of products arise from the initial formation of an energised NCOO complex with $NO + CO$ being formed in the exit channel by a 'roaming' mechanism.[45] The barrier for the direct formation of $NO + CO$ *via* a four-centre transition state is apparently too high for such a mechanism to be significant.[45]

The overall kinetics of this reaction have been studied experimentally over an exceedingly wide range of temperature. Thus, in some of the earliest CRESU

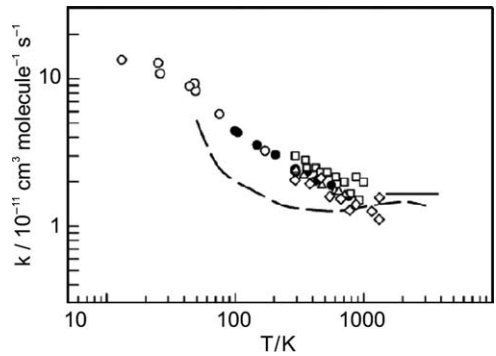

Figure 1.6 Comparison of the experimental rate coefficients for the $CN + O_2$ reaction with the theoretical results of Klippenstein and Kim.[50] The sources of the experimental data are defined in ref. 50.
(Reproduced, with permission, from ref. 50.)

(Cinétique de Réactions en Ecoulement Supersonique Uniforme) experiments,[46a,b] rate constants were measured at temperatures down to 13 K, while the kinetics have been investigated up to 4500 K in shock tube experiments.[47] The results of these studies, and several others, are displayed in Figure 1.6 and a full listing of work published by the year 2000 is given in ref. 17. As the results in Figure 1.6 show, the rate constants for the overall reaction have similar values down to 300 K, but then rise steeply to lower temperatures. The values from 295 K down to 10 K have been fitted to eqn (1.10) with $\alpha = 2.5\times10^{-11}$ cm^3 molecule^{-1} s^{-1}, $\beta = -0.63$, and $\gamma = 0$.[48]

At 13 K, long-range TST estimates the rate constant for $CN + O_2$ as 2.64×10^{-10} cm^3 molecule^{-1}, about twice the experimental value of 1.34×10^{-10} cm^3 molecule^{-1}.[16] Moreover, capture estimates at higher temperatures suggest a positive temperature-dependence of the rate constant.[49] The reaction has been examined by Klippenstein and Kim[50] using a variational version of statistical RRKM theory that was originally designed to treat 'barrierless' association reactions. They used *ab initio* electronic structure calculations to define the variation of the potential energy as the C – O separation distance in NCOO was varied between 1.7 and 3.0 Å with the NCO and COO bending angles optimised at each separation. The conserved modes such as the CN and OO vibrations, and the transitional modes such as those which correlate with the CN and OO rotations, were treated separately. The partition functions for the former motions were treated in the standard manner for harmonic oscillators, whereas those for the transitional modes were estimated *via* the corresponding phase space integrals. The reaction was assumed to occur on the lower doublet PES but not on the quartet PES which correlates with $CN(^2\Sigma^+) + O_2(^3\Sigma_g^-)$.

The results of Klippenstein and Kim[50] are compared with the experimental results in Figure 1.6. Although there are significant differences, assigned by Klippenstein and Kim to approximations in their method, the calculations reproduce the strong negative temperature-dependence of $k(T)$ at temperatures

below 298 K and the essentially constant value at higher temperatures. Their analysis also makes it clear that the dynamics of this reaction—as for the association reactions discussed earlier—are determined at inter-reactant separations where chemical forces are important. Despite the extensive work on the kinetics of radical–radical association reactions using VRC-TST referred to earlier, as far as I am aware, this theoretical method has not been applied to non-associative radical–radical reactions other than CN + O_2. It is desirable that this is done, since it is difficult to obtain experimental data for such reactions, especially at low temperatures like those in dense interstellar clouds where they may play an important role in the chemistry.

1.4.3 Reactions between Radicals and Unsaturated Molecules

The presence of a separate section on the reactions between radicals and unsaturated molecules reflects two facts: (i) the reactions are important, or potentially important, in a number of environments, combustion systems, planetary atmospheres and interstellar clouds, and they have been widely studied; and (ii) they do not fall comfortably into the categories of unimolecular or bimolecular reactions. The reactions generally proceed *via* the initial formation of a chemically bound radical adduct, which may be collisionally stabilised or breakdown to products. The competition between different reaction channels can depend on the nature of the radical, the size and nature of the unsaturated molecule, the total pressure and the temperature.

To illustrate the complexities that may arise, the reaction between OH radicals and ethene molecules, C_2H_4, is taken as an example. The evaluation by Baulch *et al.*[17] lists five possible channels for this reaction:

$$OH + C_2H_4 \rightarrow H_2O + C_2H_3 \quad \Delta_r H^{\circ}_{298} = -31.7\text{kJmol}^{-1}; \qquad \text{(R12a)}$$

$$OH + C_2H_4 \rightarrow HCHO + CH_3 \quad \Delta_r H^{\circ}_{298} = -51.8\text{kJmol}^{-1}; \qquad \text{(R12b)}$$

$$OH + C_2H_4 \rightarrow C_2H_3OH + H \quad \Delta_r H^{\circ}_{298} = 1.49\text{kJmol}^{-1}; \qquad \text{(R12c)}$$

$$OH + C_2H_4 \rightarrow CH_3CHO + H \quad \Delta_r H^{\circ}_{298} = 113.2\text{kJmol}^{-1}; \qquad \text{(R12d)}$$

$$OH + C_2H_4(+M) \rightarrow C_2H_4OH \quad \Delta_r H^{\circ}_{298} = -125.6\text{kJmol}^{-1}; \qquad \text{(R12e)}$$

The kinetics of the overall reaction have been studied, over a range of temperatures and pressures, by observing the decay of OH radicals in the presence of known concentrations of C_2H_4. Particularly noteworthy are the experiments of Fulle *et al.*,[51] who measured the rate constant at pressures up to 150 bar of helium at temperatures between 300 and 700 K. Based on a short extrapolation, they derived a temperature-independent value of $k(T) = 1.0 \times 10^{-11}\,\text{cm}^3$ molecule^{-1} s^{-1} in the limit of high pressure. At the pressures and temperatures found in the Earth's atmosphere, channel (R12e) predominates and the

IUPAC evaluation (www.iupac-kinetic.ch.cam.ac.uk) recommends the values of:

$$k^0_{ass}(T) = 8.6 \times 10^{-29}(T/300)^{-3.1}[N_2] \text{ cm}^3 \text{ molecule}^{-1} \text{ s}^{-1} \quad (1.39)$$

$$k^\infty_{ass}(T) = 9.0 \times 10^{-12}(T/300)^{-0.85} \text{ cm}^3 \text{ molecule}^{-1} \text{ s}^{-1} \quad (1.40)$$

for the rate constants in the limits of low and high pressure; the former expression for the range 200–300 K, the latter for 100–500 K. At temperatures at and above *ca.* 700 K, the C_2H_4OH adduct decomposes to the products of reactions (R12b), (R12c) and (R12d), although the branching ratios have not been established.[17]

Greenwald *et al.*[52] have applied a two transition state treatment to the addition of OH to C_2H_4. The outer transition state is treated by the long-range TST method[16] and a variational TST treatment based on high level quantum chemical estimates of the potential are applied to the inner transition state. They note that an accurate treatment of the two transition state regions at an energy and angular momentum resolved level is essential to a successful treatment of this reaction. The outer transition state exerts a dominant effect on the dynamics below 130 K, the inner transition state above 130 K. The calculated rate constants are in good agreement with the experimental values, but show a rather complex dependence on temperature which, between 10 and 600 K, can be fitted to the expression:

$$\begin{aligned} k(T) = {} & 4.93 \times 10^{-12}(T/298)^{-2.488}\exp(-53.8/T) + 3.33 \\ & \times 10^{-12}(T/298)^{0.451}\exp(-59.2/T) \text{ cm}^3 \text{ molecule}^{-1} \text{ s}^{-1} \end{aligned} \quad (1.41)$$

The kinetics of the reactions of several atomic and molecular free radicals with alkenes and alkynes have been studied down to low temperatures in CRESU experiments.[53] The results of these experiments have been reviewed and analysed by Smith *et al.*[54] Based on semi-empirical arguments, as well as correlations of room temperature rate constants, they suggested which reactions of radicals with unsaturated molecules are likely to be fast at *ca.* 10 K, that is, the temperatures found in the cold cores of dense interstellar clouds.

The semi-empirical arguments deployed explained correlations between the rate constants and changes in the quantity (*I.E.* − *E.A.*), where *I.E.* is the ionisation energy of the molecule and *E.A.* the electron affinity of the radical. The basic premise of this approach is that, where there is a barrier on the MEP for a reaction, it can be viewed as an avoided crossing between two PESs—one correlating with the ground electronic state of the separated reactants but an excited state of the products, the other correlating with the ground electronic state of the separated products and an excited, usually ionic, state of the reactants. The correlations examined by Smith *et al.*[54] suggest that if (*I.E.* − *E.A.*) is less than *ca.* 8.75 eV, the barrier is submerged and the rate constant for reaction will be large, especially at low temperatures.

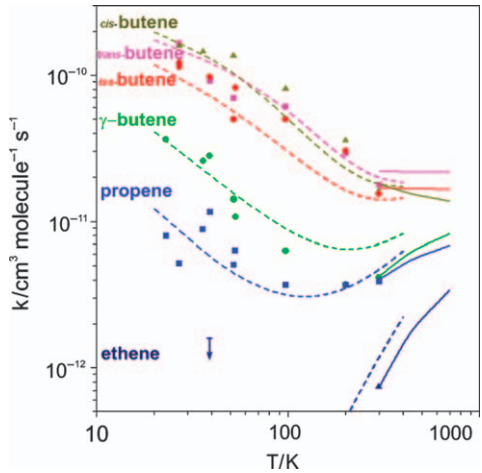

Figure 1.7 Low temperature rate coefficients for the reaction of $O(^3P)$ atoms with alkenes compared with theoretical results based on the two transition state approach.
(Reproduced, with permission, from ref. 55.)

Smith *et al.*[54] pointed out that the values of $(I.E. - E.A.)$ for reactions of $O(^3P)$ with alkenes straddle the critical value of 8.75 eV and would therefore comprise an interesting test case for the proposals in their paper. CRESU experiments were subsequently performed on these reactions by Sabbah *et al.*[55] and their results are shown in Figure 1.7. They are compared with the results of calculations based on the two transition state model which made use of *ab initio* calculations of the potential at long and medium range. The *ab initio* calculations confirmed that all the reactions that were studied, apart from that of $O(^3P)$ with ethene, for which $(I.E. - E.A.) = 9.05$ eV, exhibit submerged barriers at separations shorter than those associated with the van der Waals minima. As the curves in Figure 1.7 show, the agreement of theory with experiment is excellent.

1.5 Concluding Remarks

In this chapter I have sought to show that the temperature-dependence of the rate constants for elementary reactions are frequently not well-matched by the simple Arrhenius equation, eqn (1.2)—it could be said that we live in a 'post-Arrhenius age'. The relatively common observation of non-Arrhenius behaviour has been brought about largely by advances in experimental methods and especially the ability to measure rate constants more accurately, for a wider range of reactants and over a wider range of temperature than before. Some examples of reactions that exhibit non-Arrhenius behaviour are considered in Section 1.4.

A major emphasis in this chapter has been to examine what factors, other than a barrier along the MEP leading from reactants to products, influence the magnitude and temperature-dependence of the rate constants for elementary

reactions. Largely, I have conducted this examination through the prism of TST. Non-Arrhenius behaviour is most apparent for reactions where there is no barrier on the MEP or, at most, a barrier that is no greater than *RT*. We have seen that this is frequently the case for several classes of reaction: (i) those between ions and molecules; (ii) those between radicals and unsaturated molecules; and (iii) those between pairs of free radicals. The rate constants for many such reactions are determined either by passage through long-range ('outer') transition states, where the forces between reactants are those arising from van der Waals' forces, or by the combined influence of these outer transition states and inner transition states where chemical forces act and a submerged barrier may be present. To treat such reactions properly by TST, and to find thermal rate constants, it is necessary to calculate rate coefficients for defined energies and angular momentum and then to take averages appropriate to the temperatures of interest.

There is still relatively little information about the kinetics of non-associative reactions between radicals, especially at other than room temperature, and this presents a challenge to both experimentalists and theoreticians. The paucity of information reflects the difficulty in making kinetic measurements on such reactions when they involve two reactive radicals. In addition to hoping that more such measurements will be made, it is also desirable that the kind of calculations carried out by Klippenstein and Kim[50] on the $CN + O_2$ reaction are extended to other radical–radical systems. It will be necessary to calculate the intermolecular potentials at long- and medium-range with high accuracy, and then to find the partition functions associated with motions orthogonal to the MEP. A further difficulty, where both reactants are not in S or Σ electronic states, will be to allow properly for the coupling between the nearly degenerate PESs which correlate with the reactants. Such calculations on radical–radical reactions could provide important information about rate constants for reactions that are included in data bases for interstellar chemistry, like KIDA.[48]

Finally, I point out an important omission—largely through lack of space. A number of reactions, especially between radicals occur over 'multiwell potentials', like that between NH_2 and NO, for which the variation of potential energy along the MEP was shown in Figure 1.2. The kinetics of such reactions can require special treatment,[56] especially if there are competing pathways.

Acknowledgements

The author is grateful to Dr Stephen Klippenstein for very helpful comments on the initial draft of this article and to Dr Peter Barnes for help in preparing the diagrams.

References

1. K. J. Laidler, *J. Chem. Educ.*, 1984, **61**, 494.
2. J. H. Van t'Hoff, *Etudes de dynamique chimique*, F. Muller & Co., Amsterdam, 1884.

3. L. Pfaundler, *Ann. Phys. Chem.*, 1867, **131**, 55.
4. S. Arrhenius, *Z. Phys. Chem.*, 1889, **4**, 226.
5. D. M. Kooij, *Z. Phys. Chem.*, 1893, **12**, 155.
6. (a) R. C. Tolman, *J. Am. Chem. Soc.*, 1920, **42**, 2506; (b) R. C. Tolman, *The Principles of Statistical Mechanics*, Clarendon Press, Oxford, 1938.
7. I. W. M. Smith, *Chem. Soc. Rev.*, 2008, **37**, 812.
8. F. J. Aoiz, L. Banares and V. J. Herrero, *J. Chem. Soc. Faraday Trans.*, 1998, **94**, 2483.
9. A. González-Lafont, T. N. Truong and D. G. Truhlar, *J. Phys. Chem.*, 1991, **95**, 4618.
10. A. Fernandez-Ramos, J. A. Miller, S. J. Klippenstein and D. G. Truhlar, *Chem. Rev.*, 2006, **106**, 4518.
11. S. Chapman, S. M. Hornstein and W. H. Miller, *J. Amer. Chem. Soc.*, 1975, **97**, 893.
12. I. W. M. Smith, *Kinetics and Dynamics of Elementary Gas Reactions*, Butterworths, London, 1980.
13. (a) D. G. Truhlar, A. D. Isaacson and B. C. Garrett, in *Theory of Chemical Reaction Dynamics*, vol. 4, ed. M. J. Baer, CRC Press, Boca Raton, FL, 1985, ch. 2, pp. 65–137; (b) I. W. M. Smith, *Acc. Chem. Res.*, 1990, **23**, 101.
14. V. Wakelam, I. W. M. Smith, E. Herbst, J. Troe, W. Geppert, H. Linnartz, K. E. Roueff, M. Agundez, P. Pernot, H. M. Cuppen, J. C. Loison and D. Talbi, *Space Sci. Rev.*, 2011, **49**, 29.
15. I. W. M. Smith, *Ann. Rev. Astronom. Astrophys*, 2011, **49**, 29.
16. Y. Georgievskii and S. J. Klippenstein, *J. Chem. Phys.*, 2005, **122**, 194103.
17. D. L. Baulch, C. T. Bowman, C. J. Cobos, R. A. Cox, T. Just, J. A. Kerr, M. J. Pilling, D. Stocker, J. Troe, W. Tsang, R. W. Walker and J. Warnatz, *J. Phys. Chem. Ref. Data*, 2005, **34**, 757.
18. J. A. Miller and S. J. Klippenstein, *J. Phys. Chem. A*, 2000, **104**, 2061.
19. F. W. Schneider and B. S. Rabinovitch, *J. Amer. Chem. Soc.*, 1962, **84**, 4215.
20. See Table 7.35 on page 250 in P. J. Robinson and K. A. Holbrook, *Unimolecular Reactions*, Wiley-Interscience, London, 1972.
21. M. Quack and J. Troe, *Ber. Bunsenges. Phys. Chem*, 1974, **78**, 240.
22. J. Troe, *J. Chem. Phys.*, 1981, **75**, 226.
23. J. Troe, *J. Chem. Phys*, 1977, **66**, 4745–4758.
24. (a) H. Harrison, H. S. Johnston and E. R. Hardwick, *J. Amer. Chem. Soc.*, 1962, **84**, 2478; (b) K. Glanzer and J. Troe, *Ber. Bunsenges. Phys. Chem*, 1974, **78**, 71; (c) M. S. Woolridge, R. K. Hanson and C. T. Bowman, in *Shock Waves in Marseilles II*, ed. R. Brun and L. Z. Dumitrescu, Springer-Verlag, Berlin, 1995, pp. 83–88.
25. A. K. Mollner, S. Valluvadasan, L. Feng, M. K. Sprague, M. Okumura, D. B. Milligan, W. J. Bloss, S. P. Sander, P. T. Martien, R. A. Harley, A. B. McCoy and W. P. L. Carter, *Science*, 2010, **330**, 646.
26. (a) D. Fulle, H. F. Hamann, H. Hippler and J. Troe, *J. Chem. Phys.*, 1998, **108**, 5391; (b) H. Hippler, S. Nasterlack and F. Striebel, *Phys. Chem. Chem. Phys.*, 2002, **4**, 2959.

27. (a) J. Troe, *Int. J. Chem. Kinet.*, 2001, **33**, 878; (b) J. Troe, *J. Phys. Chem. A*, 2012, **116**, 6387.
28. NASA Panel for Data Evaluation, *Chemical Kinetics and Photochemical Data for Use in Atmospheric Studies*, Evaluation Number 17, JPL Publication 10-6, National Aeronautics and Space Administration, Jet Propulsion Laboratory, Pasadena, CA, 2011.
29. S. J. Klippenstein and L. B. Harding, *J. Phys. Chem. A*, 1999, **103**, 9388.
30. Y. Georgievskii, J. A. Miller and S. J. Klippenstein, *Phys. Chem. Chem. Phys.*, 2007, **9**, 4259.
31. L. B. Harding, Y. Georgievskii and S. J. Klippenstein, *J. Phys. Chem. A*, 2005, **109**, 4646.
32. S. J. Klippenstein, *J. Chem. Phys.*, 1992, **96**, 367.
33. L. B. Harding, S. J. Klippenstein and A. W. Jasper, *Phys. Chem. Chem. Phys.*, 2007, **9**, 4055.
34. L.-P. Ju, K.-L. Han and J. Z. H. Zhang, *J. Theor. Comput. Chem.*, 2006, **5**, 769.
35. M. A. Ter Horst, G. C. Schatz and L. B. Harding, *J. Chem. Phys.*, 1996, **105**, 558.
36. L.-P. Ju, T.-Z. Xie, K.-L. Han and J. Z. Zhang, *Chem. Phys. Lett.*, 2005, **409**, 249.
37. D. S. Wang and J. M. Bowman, *J. Chem. Phys.*, 1994, **101**, 8646.
38. J. C. Polanyi, *Acc. Chem. Res.*, 1972, **5**, 161.
39. I. R. Sims, J. L. Queffelec, D. Travers, B. R. Rowe, L. Herbert, J. Karthauser and I. W. M. Smith, *Chem. Phys. Lett.*, 1993, **211**, 461.
40. R. J. Balla, K. H Castleton, J. S. Adams and L. Pasternak, 1991, **95**, 8694 .
41. Y. Georgievskii and S. J. Klippenstein, *J. Phys. Chem. A*, 2007, **111**, 3802.
42. (a) D. Talbi and I. W. M. Smith, *Phys. Chem. Chem. Phys.*, 2009, **11**, 8477; (b) M. A. Blitz, P. W. Seakins and I. W. M. Smith, *Phys. Chem. Chem. Phys.*, 2009, **11**, 10824.
43. M. A. Blitz, D. Talbi, P. W. Seakins and I. W. M. Smith, *J. Phys. Chem. A*, 2012, **116**, 5877.
44. W. Feng and J. F. Hershberger, *J. Phys. Chem. A*, 2009, **113**, 3523.
45. F. Mohammad, V. R. Morris, W. H. Fink and W. M. Jackson, *J. Phys. Chem.*, 1993, **97**, 11590.
46. (a) I. R. Sims, J. L. Queffelec, A. Defrance, C. Rebrion-Rowe, D. Travers, B. R. Rowe and I. W. M. Smith, *J. Chem. Phys.*, 1992, **97**, 8798; (b) I. R. Sims, J. L. Queffelec, A. Defrance, C. Rebrion-Rowe, D. Travers, P. Bocherel, B. R. Rowe and I. W. M. Smith, *J. Chem. Phys.*, 1994, **100**, 4229.
47. D. F. Davidson, A. J. Dean, M. D. DiRosa and R. K. Hanson, *Int. J. Chem. Kinet.*, 1991, **23**, 1035.
48. KIDA (KInetic Database for Astrochemistry), http://kida.obs.u-bordeaux1.fr (accessed 16 May 2013).
49. T. Stoecklin, C. E. Dateo and D. C. Clary, *J. Chem. Soc. Faraday Trans.*, 1991, **87**, 1667.
50. S. J. Klippenstein and Y. W. Kim, *J. Chem. Phys.*, 1993, **99**, 5790.

51. D. Fulle, H. F. Hamann, H. Hippler and C. P. Jansch, *Ber. Bunsenges. Phys. Chem*, 1997, **101**, 1433.
52. E. E. Greenwald, S. W. North, Y. Georgievskii and S. J. Klippenstein, *J. Phys. Chem. A*, 2005, **109**, 6031.
53. I. W. M. Smith, *Angew. Chem. Int. Ed.*, 2006, **45**, 2842.
54. I. W. M. Smith, A. M. Sage, N. M. Donahue, E. Herbst and D. Quan, *Faraday Discuss.*, 2006, **133**, 137.
55. H. Sabbah, L. Biennier, I. R. Sims, Y. Georgievskii, S. J. Klippenstein and I. W. M. Smith, *Science*, 2007, **317**, 102.
56. J. A. Miller, S. J. Klippenstein, S. H. Robertson, M. J. Pilling and N. J. B. Green, *Phys. Chem. Chem. Phys.*, 2009, **11**, 1128, and references therein.